Desalination and Water Treatment
www.deswater.com

doi: 10.1080/19443994.2015.1010229

57 (2016) 6063–6071
March

Taylor & Francis
Taylor & Francis Group

Dye removal by incineration residues of pharmaceutical wastes in aqueous solution

K. Khelif*, Z. Salem, L. Boumehdi

Laboratory of Industrial Process Engineering Sciences (LSGPI), Faculty of Mechanical and Process Engineering, University of Sciences and Technology Houari Boumediene, BP 32 El-Alia-Bâb-Ezzouar, 16 311 Algiers, Algeria, Tel. +213 0771173428; email: khe.khadidja@hotmail.fr (K. Khelif), Tel. +213 0663054208; email: zsalem141@gmail.com (Z. Salem)

Received 6 February 2014; Accepted 11 January 2015

ABSTRACT

The batch removal of Basic Red 46 (BR 46) from aqueous solution using low-cost adsorbents, such as incineration residues (IR) of pharmaceutical wastes, under different experimental conditions was investigated in this study. The effects of initial BR 46 concentration (10, 25, 50, 75, and 100 mg L^{-1}), amount of residues C_S (10, 15, 20, 30, and 40 g L^{-1}), pH (3, 5, 7, 9, and 11), and temperatures T (284, 293, 306, 316, and 346 K) have been reported. Adsorption of BR 46 is highly dependent on the initial pH, the amount of adsorbent, and temperature. Results showed that BR 46 removal increased up to 94%. The adsorption phenomenon governing this process was best described by the Langmuir. Equilibrium data fitted well with the Langmuir isotherm model. The monolayer sorption capacity was found as 12.04 mg g^{-1}. A comparison of kinetic models applied to the adsorption of BR 46 on the adsorbent was evaluated for the pseudo-first-order and the pseudo-second-order. Results show that the pseudo-second-order kinetic model was found to correlate perfectly with the experimental data. The activation energy for BR 46 sorption onto the IR was found to be 30.53 kJ mol^{-1}, indicating a physical process. The adsorption of BR 46 was endothermic and spontaneous. From the experimental results, it may be concluded that IRPW seems to be an efficient and economical adsorbent for BR 46 removal.

Keywords: Adsorption; Basic Red 46; Incineration residues; Equilibrium isotherm; Thermodynamic

1. Introduction

Industrial effluents contain several non-biodegradable substrates that can be harmful to the environment [1]. One major source of these effluents is the waste arising from the industrial process, which utilizes dyes to color paper, plastic, natural, and artificial fibers [2]. A substantial amount of dyestuff is lost during the dyeing process in the textile industry [2], which poses a major problem for the industry as well as a threat to the environment [2,3]. Decolorization of dye effluents has therefore acquired increasing attention.

Due to the complex structure and stability of dyes, conventional biological treatment methods are

*Corresponding author.

Presented at the 3rd Annual International Conference on Water (CI.EAU2013), 18–20 November 2013, Algiers, Algeria

ineffective [4–7]. Moreover, their removal from wastewater by conventional coagulation, membrane filtration, and activated sludge processes is difficult, since reactive dyes are highly soluble in water [8]. These processes have considerable energy requirements and thus, impose high economic and environmental costs [4,9,10].

Therefore, alternative simple methods to work alongside these are sought. Sorption is known to be a promising technique, which has great importance due to ease of operation and comparable low cost of application in treating textile dyeing effluents [7,10]. Adsorption, as one of the most economical promising techniques, has been used extensively in removing some toxic waste present in water. Adsorbent materials, as the key factor in adsorption technology, should be attracted with much attention. Activated carbon undoubtedly is known and regarded as the most popular adsorbent, and has been widely used in wastewater treatment. But, its higher cost of manufacturing and regeneration limit its large-scale application.

So far, different adsorbents such as fly ash and lignite [11], sawdust [12–14], barley husk [15], peat [16], silica [17], activated carbon [18–20], soya cake [21], and hardened paste of Portland cement [22] have been found in literature.

Incineration residues (IR) (fly and bottom ashes) have received our particular attention as a potential adsorption material because of its low cost and availability. These two residues in dye effluents treatment will manage a greater amount of incineration wastes.

The main focus of this study was to evaluate the dye biosorption capacity by the IR, and to evaluate the effects of adsorption time, adsorbent dosage, pH, and temperature. Moreover, kinetic and equilibrium models were used to fit experimental data, physical and chemical studies were carried out to determine the mechanisms involved in the biosorption process.

2. Material and method

The basic dye used as adsorbate in the present study was 1H-1,2,4-triazolium, 1,4-dimethyl-5-[[4-[methyl(phenylmethyl)amino]phenyl]azo], and chloride. ($C_{18}H_{23}ClN_6$; MW = 357.5 g mol^{-1}, λ_{max} = 530 nm) [22]. The dye stock solution was prepared by dissolving accurately weighted amounts of dye in 1,000 mL deionized water, and the experimental solutions were obtained by diluting the stock solution to the required concentrations.

IR of pharmaceutical products wastes were obtained from incineration unit of Algiers (ECFERAL). This material was reduced by crushing and then screened through a set of sieves to get particle size (Sp) between 100 and 250 μm. No other chemical or physical treatments were used prior to sorption experiments. Chemical composition of this material was defined using X-ray fluorescence (Niton XL3T GOLDD). The surface functional groups were detected by Fourier transform infrared (FTIR) spectroscope. The specific surface area was determined using Brunauer–Emmett–Teller nitrogen gas sorption method, and which gave the value of 3.5 m^2 g^{-1}.

For kinetic studies, adsorption experiments were carried out by shaking an adsorbent dose (C_s) with aqueous solutions of 500 mL of the RB 46 in 1,000 mL-Erlenmeyer flasks at different concentrations (C_0), pHs, and temperatures (T) as a function of time.

The effects of varying the IR mass (C_s) on dye adsorption were carried out by adding 10, 15, 20, 30, and 40 g L^{-1} samples of IR to 1,000 mL solution of Basic Red (BR46) aqueous solution 50 mg L^{-1}as initial concentration.

The initial dye concentration (C_0) was investigated as follows: 10 g sample of IR was added to 1,000 mL solution of BR46 with initial concentrations varying from 10 to 100 mg L^{-1}.

Effect of initial pH was investigated for various pH values, which are 3, 5, 7, 9, and 11. The pH was adjusted to a given value by the addition of HCl (1 mol L^{-1}) or NaOH (1 mol L^{-1}) and was measured using Hanna HI-8224 pH-meter.

After the desired contact time, the samples were withdrawn from mixture by means of a micropipette, and then they were centrifuged for 2 min at 6,000 rpm. The concentrations of dyes were determined from its UV–Vis absorbance characteristic with the calibration method. Using a Shimadzu UV-1800 visible spectrophotometer. A linear correlation was established between the dye concentration and the absorbance at λ_{max} = 530 nm, in the dye concentration range 0–20 mg $L^{-1}$with a correlation coefficient R^2 = 0.997.

Before starting the adsorption tests, we run a blank with no adsorbent in the reactor. There is no significant adsorption on the walls of the reactor.

The BR 46 amount adsorbed by IR was calculated using the mass balance by using following equation

$$q_{ads} = \left(\frac{C_0 - C_e}{m}\right) \times V_L \quad (1)$$

The BR 46 removal (%) was calculated using by using following equation:

$$\mathrm{Re}(\%) = \left(\frac{C_0 - C_e}{C_0}\right) \times 100 \quad (2)$$

where q_{ads} is BR 46 amount adsorbed on IR (mg g^{-1}), C_0 and C_e are, respectively, the initial and final BR 46 concentrations (mg L^{-1}), V is solution volume (L), and m is the adsorbent weight (g).

3. Results and discussion

3.1. IR characterization

Chemical composition of IR obtained from expired pharmaceuticals (raw ashes) was defined using X-ray fluorescence (Niton XL3T Goldd). The obtained results are summarized in Table 1.

The chemical composition of IR shows that calcium is the major component. The other analyzed heavy metals are found in trace amounts. The metal contents in IR are compared with the limit values for sludge use in agriculture and with wastes admissions criteria in sanitary landfill. They are well below the standards. Samples of IR were also submitted to the neutral test water (according to AFNOR X31-210), which simulates landfill solid wastes exposed to neutral pH. The residue showed a strong alkaline property with pH 9.98. The results obtained show that the IR does not represent a potential danger for the environment.

3.2. Infrared spectral analysis

To know the nature of the functional groups responsible for dye sorption, infrared spectrum has been established. Fig. 1 gives the FTIR spectra of incineration residue. It presents several absorption peaks indicating complex adsorbent structure. This analysis shows broadband at 3,452 cm^{-1} representing bonded −OH groups, which corresponds to the alcohols and acids carboxylic. The peaks observed at 2,843 and 2,915 cm^{-1} correspond to $–CH_2$ and –CH groups. Another vibration peak was detected at 1,627 cm^{-1} related to the carbonyl groups COO^-. The spectra presents also a peak at 1,424 cm^{-1} related to C–H, –C–O, N–H, and C–N stretching groups. The peak located at 1,084 cm^{-1} is related probably to several stretching groups (–C–O, –OH, N–H, C–N, S=O, C–F, and C–Cl). The peak at 876.71 cm^{-1} presents halogen stretching.

3.3. Batch sorption studies

The effects of contact time, adsorbent dose, pH, and temperature on BR 46 removals from aqueous solution by IR have been studied to optimize the process.

3.3.1. Effect of contact time and adsorbent dose on BR 46 removal

The contact time effect on BR 46 removal is shown in Fig. 2. The sorption performance increases rapidly reaching 47.34% in the first hour and saturation occurs at about 270–330 min.

The fast adsorption at initial stage could be due to the fact that a large number of active sites are available responsible for sorption of BR 46 on the IR. After the rapid diffusion of dye molecules from the bulk solution to the exterior surface of adsorbent particles, the removal rate slowed down gradually until the equilibrium. This could be a consequence of saturation of active sites in exterior surface and entrance of dye molecules into the adsorbent pores [23]. This tendency is an agreement with results obtained by previous studies with sorption of Reactive Red 120 on natural untreated clay [24].

Table 1
Elemental composition of raw IR

Elements	Amount in ICPW (mg Kg^{-1})	Metal limit value for agricultural sludge (mg Kg^{-1})	Elements	Amount in ICPW (mg Kg^{-1})	Metal limit value for agricultural sludge (mg Kg^{-1})
Hg	Trace	10	Fe	1.0798	–
Ni	0.3599	200	Mn	0.4756	–
As	Trace	–	Cr	1.2273	1,000
Cd	Trace	20	Ti	1.8417	–
Zn	0.7757	3,000	Ca	5.5239	–
Cu	0.0683	1,000	K	0.0425	–
Sn	0.1157	–	S	0.1758	–
Pb	0.0412	800	Sr	0.0108	–
Zr	0.1531	–	Rb	0.0009	–

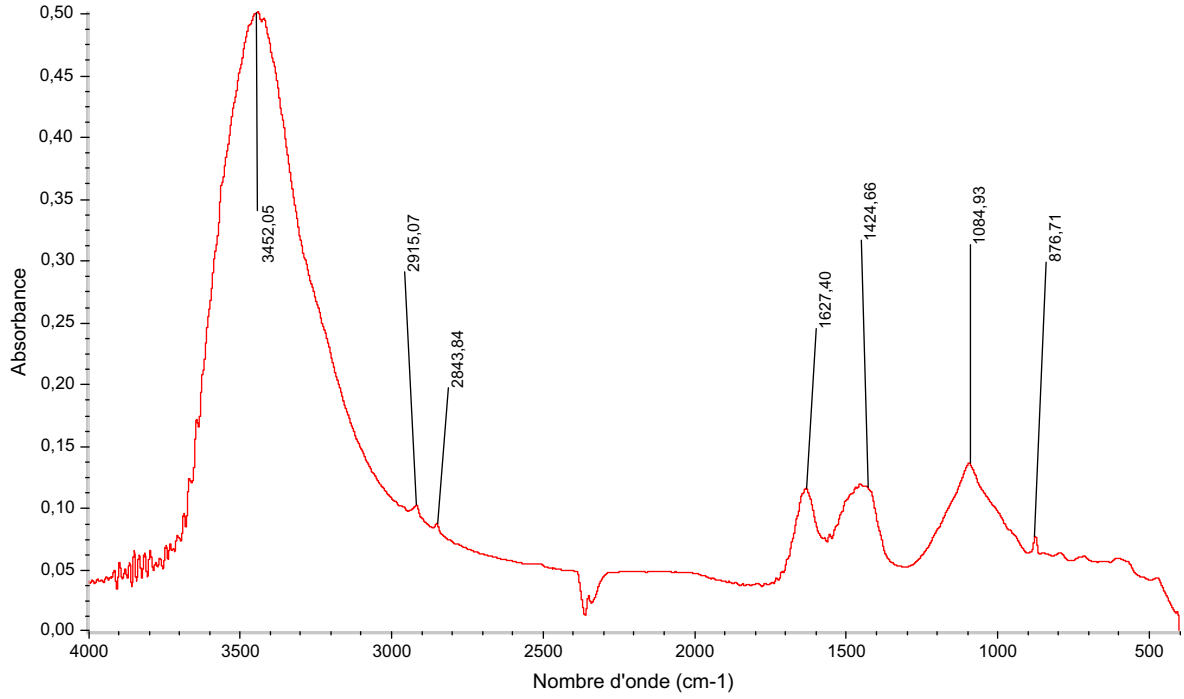

Fig. 1. Infrared spectral analysis of IR.

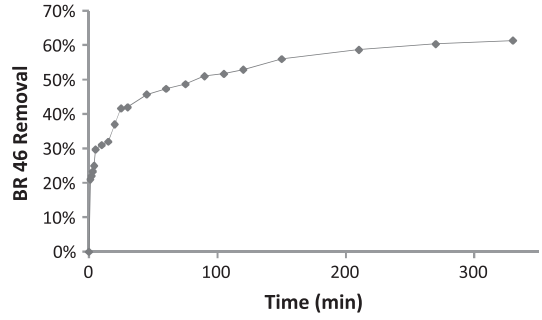

Fig. 2. Effect of contact time on BR 46 adsorption (C_0 = 50 mg L^{-1}, C_s = 10 g L^{-1}, N = 300 rpm, pH = 9.48, and T = 295.5 K).

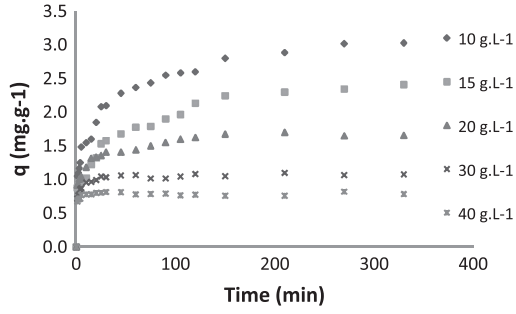

Fig. 3. Effect of adsorbent dose on BR 46 adsorption (C_s = 10 g L^{-1}, N = 300 rpm, pH = 9.95, and T = 293 K).

These curves (Fig. 3) show that the increase of adsorbent mass drops the adsorption capacity. Retention BR 46 is maximum for small amounts of IR. This is due to an increase in free surface area of the particles for small quantities. Indeed, the decrease in the IR concentration, result a greater dispersion of particles in the aqueous phase. Therefore, the adsorbent surfaces are more exposed. This facilitates accessibility for a large number of free sites on the carrier molecules of BR 46.

Similar result was also found for the sorption of textile dyes onto cupuassu shell [25], removal of Lanaset Red G on macro-algae powder [26] and the removal of Reactive Red 120 on *Chara contraria* [23].

3.3.2. Effect of pH and temperature on BR 46 removal

Solution pH has been recognized as one of the most important factor affecting sorption process, due to its influence on surface charge of adsorbent and dye solubility [25,27]. BR 46 removal by IR as a function of pH value was investigated (Fig. 4). It appeared that the removal by sorption is influenced by the pH value, which changes the ionic charge of the adsorbent surface. In fact the amount adsorbed increases with

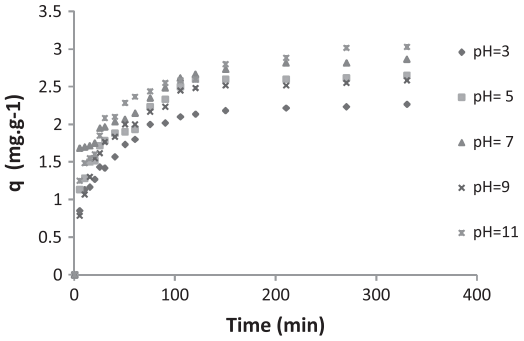

Fig. 4. Effect of pH on BR 46 adsorption (C_s = 10 g L^{-1}, C_0 = 50 mg L^{-1}, N = 300 rpm, and T = 291 K).

increasing pH from 3 to 11. This is related to the pH of point of zero charge of IR which is 9. For higher pH, the surface is negatively charged, while at pH below 9, the surface is positively charged. For high pH, the number of active negatively charged sites increases, which is due to the electrostatic attraction between the BR 46 (cationic) positively charged and negatively charged surface residues.

These results are consistent with those found by Saadatjou et al. [22] on the adsorption of BR 46 on activated carbon (pH = 10). This work confirms that the basic dyes are better adsorbed in alkaline environments.

The effect of solution temperature on dye removal (Fig. 5) was studied for five temperatures (284, 293, 306, 316, and 346 K). We can see from the results that the increase in temperature favors dye retention. The equilibrium adsorption capacity increases with solution temperature to a removal efficiency up to 88%, indicating that the process is endothermic. Acemioglu [28] study with fly ash on Congo red confirms the result with maximum efficiency at 323 K. However, the influence of temperature limits diffusion of dye molecules in the IR since the adsorbed amounts is close to equilibrium residues. A temperature of 306 K was chosen as an optimal.

3.3.3. Effect of initial dye concentration

In order to evaluate effects of initial dye concentration on the adsorption process, experiments were carried out at different initial dye concentrations (C_0 between 10 and 100 mg L^{-1}) under the operating variables (10 g L^{-1} adsorbent dose, pH 9.95, and for temperature 293 K). Effect of initial dye concentrations on the sorption is shown in Fig. 6.

Results indicated that dye sorption increased significantly with increasing initial dye concentration to reach 5.33 mg g^{-1} corresponding to 94% of dye removal, after 390 min, and for a concentration of 100 mg L^{-1}. This could be a consequence of increase in the driving force for mass transfer with increasing dye concentration. These results are in agreement with previous adsorption studies of Çelekli et al. [6], Chowdhury et al. [29] and Wang et al. [30], who have used respectively *Spirogyra majuscula* to removal reactive red 120, *Ananas comosus* leaf powder to eliminate Basic Green 4 and activated carbon prepared from *Polygonum orientale* Linn to reduce basic dyes.

3.3.4. Dye adsorption isotherms

Adsorption isotherm is basically important to describe how solutes interact with adsorbents, and it is also crucial in optimizing the adsorbent usage. The adsorption isotherm equilibrium of BR 46 on IR was tested by Langmuir and Temkin models. The applicability of the isotherm equation to the studied adsorption was evaluated by the correlation coefficients R^2. The Langmuir isotherm (Fig. 7) model can be expressed as:

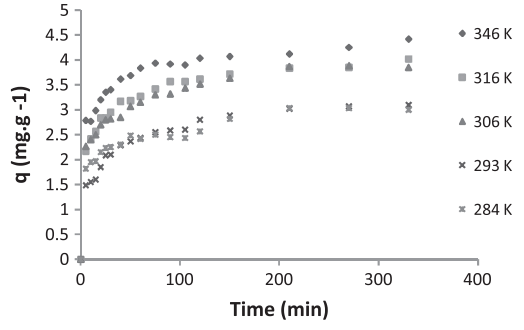

Fig. 5. Effect of temperature on BR 46 adsorption (C_s = 10 g L^{-1}, C_0 = 50 mg L^{-1}, and N = 300 rpm).

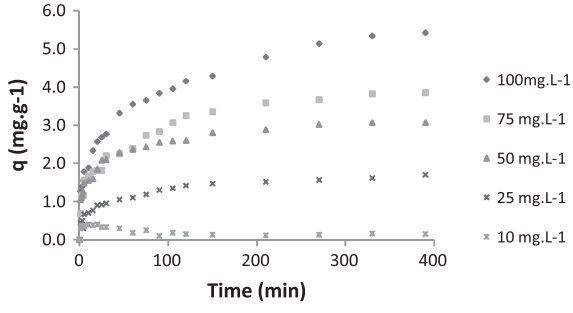

Fig. 6. Effect of initial dye concentration on (BR 46) adsorption (C_s = 10 g L^{-1}, N = 300 rpm, pH = 9.95, and T = 293 K).

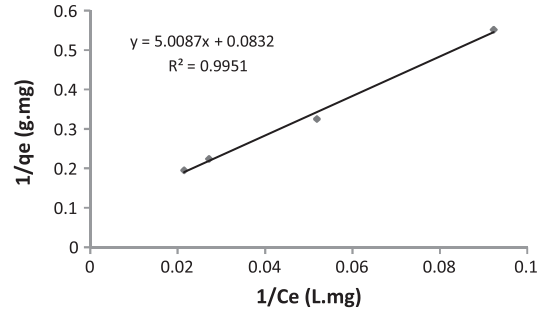

Fig. 7. Langmuir adsorption isotherm of BR 46 on IR.

$$\frac{1}{q_e} = \frac{1}{q_m} + \frac{1}{q_m b C_e} \tag{3}$$

where q_m (mg g^{-1}) and b (L mg^{-1}) are Langmuir constants related to adsorption capacity and adsorption energy, respectively. Temkin isotherm (Fig. 8) usually gives curve fitting over a wider adsorbate concentration range. It can be expressed as:

$$\ln q_e = \frac{RT}{b_T} \ln(AC_e) \tag{4}$$

from this equation, Temkin constants A and b_T can be calculated from the plot of q_e vs. ln C_e.

This model is based on the assumption that the binding energy decreases linearly with increasing saturation of the adsorbent surface [31] (see Table 2).

According to the closest coefficient of correlation to 1 the Temkin isotherm provided the best model with R^2 of 0.998. The Temkin constant R_L (~0.2) tends to zero, which shows that the adsorption is favorable and the adsorption is monomolecular.

The maximum adsorption capacity of the BR 46 on the IR found in this study is 12.04 mg g^{-1}. This result is close to those of Laasri et al. [32] who worked on two IR and found 20.47 mg g^{-1} for the fir sawdust and 19.24 mg g^{-1} for beech sawdust.

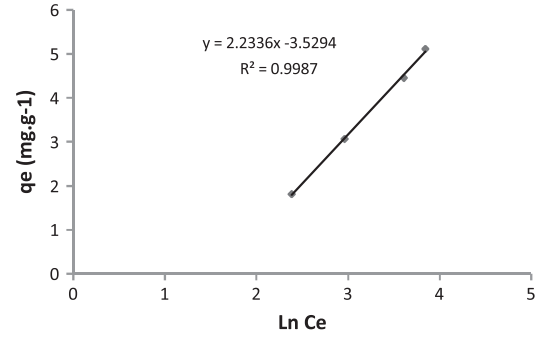

Fig. 8. Temkin adsorption isotherm of BR 46 on IR.

3.4. Adsorption kinetic

The adsorption process of porous adsorbents is controlled by three steps: liquid film diffusion, intraparticle diffusion, and chemical reaction. The study of uptake kinetics is significant as it provides valuable insights into the reaction pathway and describes the solute uptake rate, which controls the residence time of adsorbate uptake at the solid-solution interface [33]. To investigate the exchange process of BR 46 by the IR, Lagergren pseudo-first-order, and pseudo-second-order kinetic models were used to test the experimental data. The Lagergren pseudo-first-order and pseudo-second-order models are, respectively, described by using following equations:

$$\ln(q_e - q_t) = \ln(q_e) - k_1.t \tag{5}$$

$$\frac{t}{q_t} = \frac{1}{k_2 q_e^2} + \frac{t}{q_e} \tag{6}$$

where q_e and q_t are, respectively, the BR 46 amounts adsorbed on the IR (mg g^{-1}) at equilibrium and at time t, the values K_1 (min^{-1}) and K_2 (g mg^{-1} min^{-1}) are the rate constants of both pseudo-first and second-order models.

The obtained results are listed on Table 3, the pseudo-second-order rate equation for BR 46 sorption on IR agreed well with the results ($R^2 \geq 0.99$).

Researchers found that if reaction is controlled by ion exchange, the pseudo-second-order model has best fit with the experimental data [34].

3.5. Thermodynamic parameters of adsorption

The thermodynamic parameters are calculated from the following relationship:

$$\Delta G^\circ = -RT \ln K_c \tag{7}$$

$$K_c = \frac{(C_0 - C_e)}{C_e} \tag{8}$$

$$\ln K_c = \frac{\Delta S^\circ}{RT} - \frac{\Delta H^\circ}{RT} \tag{9}$$

where K_c is the equilibrium constant, ΔH°, ΔS°, and ΔG° are, respectively, the standard enthalpy, the standard

Table 2
Constants of Langmuir, Freundlich and Temkin adsorption isotherm models

Langmuir				Temkin			Freundlich		
q_m (mg g^{-1})	R_L	K (mg L^{-1})	R^2	A (L g^{-1})	b_T	R^2	K_f	$1/n$	R^2
12.04	0.196	0.016	0.992	0.206	2.233	0.998	0.358	0.699	0.986

Table 3
Effect of dye initial concentration on the constants K_1 and K_2

Pseudo-first-order			Pseudo-second-order		
C_0 (mg L^{-1})	K_1 (min^{-1})	R^2	C_0 (mg L^{-1})	K_2 (g mg^{-1} min^1)	R^2
25	0.010	0.976	25	0.0525	0.987
50	0.011	0.970	50	0.0393	0.991
75	0.005	0.929	75	0.0198	0.988
100	0.010	0.976	100	0.0132	0.992

entropy, and the standard free energy of adsorption. The determination of these parameters is done by the plot of Eq. (9) illustrated in Fig. 9 (Table 4).

R: gas constant (8.314 JK^{-1} mol^{-1})

Negative value standard free energy shows that the adsorption is carried out favorably and spontaneous. Generally, a value of ΔG° between 0 and −20 kJ mol^{-1} is consistent with electrostatic interaction between adsorption sites and the adsorbing ion (physical adsorption), while a more negative ΔG° value ranging from −80 to −400 kJ mol^{-1} indicates that the adsorption involves charge sharing or transferring from the adsorbent surface to the adsorbing ion to form a coordinate bond (chemisorption) [34–38].

The positive value of the enthalpy obtained, suggests the endothermic nature of adsorption [23] while the positive values of the standard entropy indicate an increase in the degree of freedom (or disorder) of the adsorbed species. In general, the thermodynamic parameters indicate that the adsorption is spontaneous and endothermic.

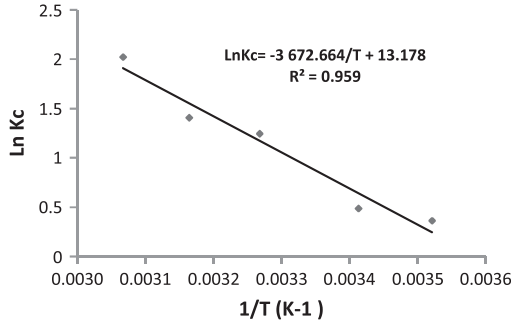

Fig. 9. Evolution of Ln K_c vs. $1/T$.

Table 4
Thermodynamic parameters values

T (K)	ΔH° (kJ mol^{-1})	ΔS° (kJ mol^{-1} K^{-1})	ΔG° (kJ mol^{-1})
284	30.5345	0.069	−0.8593
293			−1.1884
306			−3.1727
316			−3.6982
326			−5.4885

The magnitude of activation energy gives an idea about the type of sorption, which is mainly physical or chemical. Low activation energies (5–50 kJ mol^{-1}) are characteristics of physical sorption, while higher activation energies (60–800 kJ mol^{-1}) suggest chemical sorption [39]. The activation energy for BR 46 sorption onto the IR was found to be 30.53 kJ mol^{-1} indicating a physical process.

4. Conclusion

The study of the BR 46 adsorption on IR was conducted to understand the mechanism of adsorption of these molecules. It was also found that the amount adsorbed on the IR depends mainly on the initial solution pH, the amount of adsorbent, and temperature. This study showed that the IR of expired pharmaceuticals are an effective adsorbent for the removal of BR46 in aqueous solution with a dye percent elimination of 94%, despite being raw and untreated.

List of symbols

A	—	Temkin constant, L mg^{-1}
BET	—	Brunnauer–Emmet–Teller
BR 46	—	basic Red 46
b_T	—	constant relative to the adsorption heat, J mol^{-1}
C_0	—	initial solute concentration, mg L^{-1}
C_e	—	solute concentration at equilibrium, mg L^{-1}
C_s	—	concentration of incineration residues in solution, g L^{-1}
ECFERAL	—	company Boiler and Plumber ALGIERS
K_L	—	Langmuir constant, L mg^{-1}
k_1	—	rate constant for a pseudo-first-order kinetics, s^{-1}
k_2	—	rate constant for the pseudo-second-order kinetics, s^{-1}
m	—	mass of incineration residues, mg
pH	—	potential of hydrogen
PZC	—	point of zero charge
q_e	—	adsorption capacity at equilibrium, mg g^{-1}
q_m	—	maximum capacity of adsorption, mg g^{-1}
q_t	—	adsorption capacity at time t, mg g^{-1}
R	—	gas constant, J mol^{-1} K^{-1}
R^2	—	linear regression coefficient
IRPW	—	incineration residues of pharmaceutical wastes
T	—	temperature, K
V	—	solution volume V, mL
N	—	stirring velocity, rpm
ΔH°	—	the standard enthalpy, kJ mol^{-1}
ΔS°	—	the standard entropy, kJ mol^{-1} K^{-1}
ΔG°	—	the standard free enthalpy, kJ mol^{-1}
K_c	—	the equilibrium constant

References

[1] M. Qamar, M.A. Gondal, K. Hayat, Z.H. Yamani, K. Al-Hooshani, Laser-induced removal of a dye C.I. Acid Red 87 using n-type WO3 semiconductor catalyst, J. Hazard. Mater. 170 (2009) 584–589.

[2] H. Zollinger, Color Chemistry-Synthesis, Properties and Applications of Organic Dyes and Pigments, VCH Publishers, New York, NY, 1987.

[3] M. Qamar, M. Saquib, M. Muneer, Photocatalytic degradation of two selected dye derivatives, chromotrope 2B and amido black 10B, in aqueous suspensions of titanium dioxide, Dyes Pigm. 65 (2005) 1–9.

[4] A. Srinivasan, T. Viraraghavan, Decolorization of dye wastewaters by biosorbents, J. Environ. Manage. 91 (2010) 1915–1929.

[5] N. Naveen, P. Saravanan, G. Baskar, S. Renganathan, Equilibrium and kinetic modeling on the removal of Reactive Red 120 using positively charged *Hydrilla verticillata*, Chem. Eng. J. 42 (2011) 463–469.

[6] A. Çelekli, M. Yavuzatmaca, H. Bozkurt, Kinetic and equilibrium studies on biosorption of reactive red 120 from aqueous solution on *Spirogyra majuscula*, Chem. Eng. J. 152 (2009) 139–145.

[7] M. Rafatullah, O. Sulaiman, R. Hashim, A. Ahmad, Adsorption of methylene blue on low-cost adsorbents, J. Hazard. Mater. 177 (2010) 70–80.

[8] J. Paul, D.B. Naik, S. Sabharwal, High energy induced decoloration and mineralization of Reactive Red 120 dye in aqueous solution: A steady state and pulse radiolysis study, Int. J. Radiat. Phys. Chem. 79 (2010) 770–776.

[9] G. Absalan, M. Asadi, S. Kamran, L. Sheikhian, D.M. Goltz, Removal of reactive red-120 and 4-(2-pyridylazo) resorcinol from aqueous samples by Fe_3O_4 magnetic nanoparticles using ionic liquid as modifier, J. Hazard. Mater. 192 (2011) 476–484.

[10] M.A.M. Salleh, D.K. Mahmoud, W.A.W.A. Karim, A. Idris, Cationic and anionic dye adsorption by agricultural solid wastes, Desalination 280 (2011) 1–13.

[11] M. Iqbal, M.N. Ashiq, Adsorption of dyes from aqueous solutions on activated charcoal, J. Hazard. Mater. B139 (2007) 57–66.

[12] V.K. Garg, M. Amita, R. Kumar, R. Gupta, Basic dye (methylene blue) removal from simulated wastewater by adsorption using Indian Rosewood sawdust: A timber industry waste, Dyes Pigm. 63 (2004) 243–250.

[13] V.K. Garg, R. Gupta, A.B. Yadav, R. Kumar, Dye removal from aqueous solution by adsorption on treated sawdust, Bioresour. Technol. 89 (2003) 121–124.

[14] M. Ozacar, A.I. Sengil, Adsorption of metal complex dyes from aqueous solutions by pine sawdust, Bioresour. Technol. 96 (2005) 791–795.

[15] T. Robinson, B. Chandran, P. Nigam, Removal of dyes from artificial textile dye effluent by two agricultural waste residues corncob and barley husk, Environ. Int. 28 (2002) 29–33.

[16] Y.S. Ho, G. McKay, Sorption of dye from aqueous solution by peat, Chem. Eng. J. 70 (1998) 115–124.

[17] G. McKay, M.S. Otterburn, A.G. Sweeney, Surface mass transfer processes during colour removal from effluent using silica, Water Res. 15 (1981) 327–331.

[18] J.J.M. Orfao, A.I.M. Silva, J.C.V. Pereira, S.A. Barata, I.M. Fonseca, P.C.C. Faria, M.F.R. Pereira, Adsorption of a reactive dye on chemically modified activated carbons Influence of pH, J. Colloid Interface Sci. 296 (2003) 480–489.

[19] A. Jumasiah, T.G. Chuah, J. Gimbon, T.S.Y. Choong, I. Azni, Adsorption of basic dye onto palm kernel shell activated carbon: Sorption equilibrium and kinetics studies, Desalination 186 (2005) 57–64.

[20] A. Gurses, C. Dogar, S. Karaca, M. Acikyildiz, R. Bayrak, Production of granular activated carbon from waste *Rosa canina* sp. seeds and its adsorption characteristics for dye, J. Hazard. Mater. B131 (2006) 254–259.

[21] N. Daneshvar, D. Salari, S. Aber, Chromium adsorption and Cr(VI) reduction to trivalent chromium in aqueous solutions by soya cake, J. Hazard. Mater. B94 (2002) 49–61.

[22] N. Saadatjou, M.H. Rasoulifard, A. Heidari, S. Mohammad, M.D. Mohammadi, Removal of C.I. Basic Red 46 (BR 46) from contaminated water by adsorption onto hardened paste of Portland cement: Equilibrium isotherms and thermodynamic parameters study, Int. J. Phys. Sci. 6 (22) (2011) 5181–5189.

[23] A. Çelekli, G. Ilgün, H. Bozkurt, Sorption equilibrium, kinetic, thermodynamic, and desorption studies of Reactive Red 120 on *Chara contraria*, Chem. Eng. J. 191 (2012) 228–235.
[24] E. Errais, J. Duplay, F. Darragi, I. M'Rabet, A. Aubert, F. Huber, G. Morvan, Efficient anionic dye adsorption on natural untreated clay: Kinetic study and thermodynamic parameters, Desalination 275 (2011) 74–81.
[25] A. Çelekli, B. Tanrıverdi, H. Bozkurt, Predictive modeling of removal of Lanaset Red G on *Chara contraria*; kinetic, equilibrium, and thermodynamic studies, Chem. Eng. J. 169 (2011) 166–172.
[26] N.F. Cardoso, E.C. Lima, I.S. Pinto, C.V. Amavisca, B. Royer, R.B. Pinto, W.S. Alencar, S.F.P. Pereira, Application of cupuassu shell as biosorbent for the removal of textile dyes from aqueous solution, J. Environ. Manage. 92 (2011) 1237–1247.
[27] P.S. Kumar, S. Ramalingam, C. Senthamarai, M. Niranjanaa, P. Vijayalakshmi, S. Sivanesan, Adsorption of dye from aqueous solution by cashew nut shell: Studies on equilibrium isotherm, kinetics and thermodynamics of interactions, Desalination 261 (2010) 52–60.
[28] B. Acemioglu, Adsorption of Congo red from aqueous solution onto calcium-rich fly ash, J. Colloid Interface Sci. 274 (2004) 371–379.
[29] S. Chowdhury, S. Chakraborty, P. Saha, Biosorption of Basic Green 4 from aqueous solution by *Ananas comosus* (pineapple) leaf powder, Colloids Surf., B 84 (2011) 520–527.
[30] L. Wang, J. Zhang, R. Zhao, C. Li, Y. Li, C. Zhang, Adsorption of basic dyes on activated carbon prepared from *Polygonum orientale* Linn: Equilibrium, kinetic and thermodynamic studies, Desalination 254 (2010) 68–74.
[31] P. Kumar, P. Senthil, K. Kirthika, Equilibrium and kinetic study of adsorption of nickel from aquenous solution onto bael tree leaf powder, Eng. Sci. Technol. (2009) 351–363.
[32] L. Laasri, M.K. Elamrani, O. Cherkaoui, Removal of two cationic dyes from a textile effluent by filtration-adsorption on wood sawdust, Environ. Sci. Pollut. Res. 14 (2007) 237–240.
[33] M. Zhang, H. Zhang, D. Xu, L. Han, D. Niu, L. Zhang, W. Wu, B. Tian, Ammonium removal from aqueous solution by zeolites synthesized from low-calcium and high-calcium fly ashes, Desalination 277 (2011) 46–53.
[34] W.L. Zhu, L.H. Cui, Y. Ouyang, C.F. Long, X.D. Tang, Kinetic adsorption of ammonium nitrogen by substrate materials for constructed wetlands, Pedosphere 21(4) (2011) 454–463.
[35] J.M. Smith, H.C. Van Ness, Introduction to Chemical Engineering Thermodynamics, fourth ed., McGraw-Hill, Singapore, 1987.
[36] E. Malkoc, Y. Nuhoglu, Determination of kinetic and equilibrium parameters of the batch adsorption Cr(IV) onto waste acorn of *Quercusitha burensis*, Chem. Eng. Prog. 46 (2007) 1020–1029.
[37] Z.A. AlOthman, M.A. Habila, R. Ali, Kinetic, equilibrium and thermodynamic studies of cadmium (II) adsorption by modified agricultural wastes, Molecules 16 (2011) 10443–10456.
[38] M. Horsfall, A.I. Spiff, A.A. Abia, Studies on the influence of mercaptoacetic acid (MAA) modification of cassava (*Manihot sculenta* Cranz) waste biomass on the adsorption of Cu^{2+} and Cd^{2+} from aqueous solution, Bull. Korean Chem. Soc. 25 (2004) 969–976.
[39] H. Nollet, M. Roels, P. Lutgen, P. Van der Meeren, W. Verstraete, Removal of PCBs from wastewater using fly ash, Chemosphere 53 (2003) 655–665.